Dynamic Crossovers and Stepwise Solidification of Confined Water: A 2H NMR Study

ARTICLE *in* JOURNAL OF PHYSICAL CHEMISTRY LETTERS · DECEMBER 2013

Impact Factor: 7.46 · DOI: 10.1021/jz402539r

2 AUTHORS:

Matthias Sattig
Technical University Darmstadt
3 PUBLICATIONS **16** CITATIONS
SEE PROFILE

M. Vogel
Technical University Darmstadt
83 PUBLICATIONS **1,777** CITATIONS
SEE PROFILE

THE JOURNAL OF PHYSICAL CHEMISTRY Letters

Letter

pubs.acs.org/JPCL

Dynamic Crossovers and Stepwise Solidification of Confined Water: A ^{2}H NMR Study

M. Sattig and M. Vogel*

Institut für Festkörperphysik, Technische Universität Darmstadt, D-64289 Darmstadt, Germany

Supporting Information

ABSTRACT: ^{2}H NMR reveals two dynamic crossovers of supercooled water in nanoscopic (∼2 nm) confinement. At ∼225 K, a dynamic crossover of liquid water is accompanied by formation of a fraction of solid water. Therefore, we do not attribute the effect to a liquid−liquid phase transition but rather to a change from bulk-like to interface-dominated dynamics. Moreover, we argue that the α process and β process are observed in experiments above and below this temperature, respectively. Upon cooling through a dynamic crossover at ∼175 K, the dynamics of the liquid fraction becomes anisotropic and localized, implying solidification of the corresponding water network, most probably, during a confinement-affected glass transition.

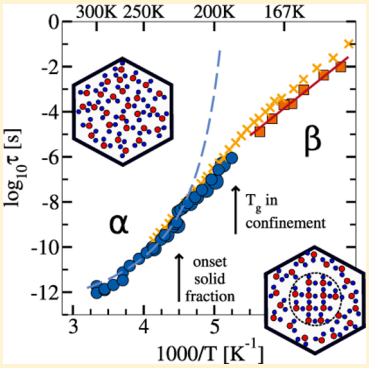

SECTION: Surfaces, Interfaces, Porous Materials, and Catalysis

Water in nanoscopic confinements is of enormous importance not only in biological and technological processes but also in fundamental research. While bulk water crystallizes in the no-man's land, 150−235 K, confined water can be kept in the liquid state in this temperature range. Liquid water in the no-man's land is of particular interest because it was proposed to exhibit a second critical point in the deeply supercooled regime, which is related to a liquid−liquid (LL) phase transition between high-density and low-density forms and brings about the water anomalies.[1,2] Despite intense research efforts, the existence of such a LL phase transition is, however, still subject to controversial scientific debate.[3] In this context, the important question arose to what extent studies on confined water enable insights into properties of bulk water as confinement results in a coexistence of interfacial and internal waters, which do and do not reside near the matrix surface, respectively, and can exhibit diverse behaviors.[4−7]

To confine water on nanoscales, MCM-41 materials proved suitable because these silica matrixes exhibit nanopores of defined and tunable diameters. Various studies focused on water in pores with diameters of ∼2.0 nm, as found, for example, in MCM-41 C10, arguing that such confinements are sufficiently large to preserve liquid behavior, while they are sufficiently small to suppress regular crystallization.[6,8] Neutron scattering (NS) studies took a kink in temperature-dependent correlation times of water dynamics at ∼225 K, as evidence for a LL phase transition.[8,9] By contrast, dielectric spectroscopy (DS) works did not observe a sharp dynamic crossover at ∼225 K but a mild one at ∼180 K, which was attributed to an interplay of the structural α relaxation and a local β relaxation,[10,11] being a potential precursor process of the former multiparticle dynamics.[3] Despite suppression of regular freezing, confined water shows calorimetric signals,[12−14] for example, enthalpy features at 180−200 and 220−250 K were attributed to formation of glassy water or distorted ice in MCM-41 C10.[14,15]

Nuclear magnetic resonance (NMR) techniques also proved to be useful tools to investigate H_2O and D_2O in MCM-41.[16] ^{1}H NMR yielded insights into pore filling and pore size,[17,18] as well as changes in structural and dynamical behaviors of confined water, which were interpreted in terms of a LL transition.[19] ^{2}H NMR provided information about both rates and mechanisms for molecular dynamics[16] as used to characterize adsorption sites at silica walls.[20,21] In addition, ^{1}H and ^{2}H NMR were employed to investigate water behaviors in other confinements.[16,22−24] Recently, we utilized ^{2}H NMR to ascertain water motion in protein matrixes over broad temperature and dynamic ranges.[25−28] Specifically, we studied spin−lattice relaxation (SLR) and performed line shape analysis (LSA) as well as stimulated echo experiments (STE).

Here, ^{2}H NMR SLR, LSA, and STE studies are combined to investigate D_2O dynamics in MCM-41 C10. The experimental setup was described in previous work.[26] MCM-41 C10, synthesized and characterized by Kittaka and co-workers,[13,29] was completely filled with D_2O from Sigma-Aldrich. It was ensured that different routes for removal of excess water do not affect the NMR results for confined water. In any case, contributions from freezable water outside of the pores are suppressed due to different SLR behavior.[25]

Received: November 22, 2013
Accepted: December 12, 2013
Published: December 12, 2013

In ^{2}H NMR, we probe the quadrupolar frequencies of ^{2}H (D) nuclei. For O−D bonds, they are approximately given by[30]

$$\omega_Q = \pm\frac{\delta}{2}(3\cos^2\theta - 1) \propto P_2(\cos\theta) \quad (1)$$

Here, $\delta \approx 2\pi\cdot 161$ kHz describes the strength of the quadrupolar interaction, and θ denotes the angle between the O−D bond and the $\mathbf{B}_0$ field. Thus, the quadrupolar frequency is proportional to the Legendre polynomial $P_2(\cos\theta)$, and fluctuations of ω_Q provide access to the associated rotational correlation function, $F_2(t)$.

First, we analyze ^{2}H SLR to study D_2O dynamics in MCM. For isotropic reorientation, the ^{2}H SLR time T_1 depends on the spectral density $J_2(\omega)$, which is related to $F_2(t)$ by Fourier transformation

$$\frac{1}{T_1} = \frac{2}{15}\delta^2[J_2(\omega_0) + 4J_2(2\omega_0)] \quad (2)$$

Here, ω_0 is the Larmor frequency. For a Debye process, $F_2(t) = \exp(-t/\tau)$ and $J_2(\omega) = \tau/(1 + \omega^2\tau^2)$, leading to a T_1 minimum for a correlation time of $\tau \approx 1/\omega_0 \approx 1$ ns.

To determine T_1, we analyze the buildup of magnetization after saturation, $M(t)$. For the confined water, the buildup is well-described by a single exponential above 223 K, while two relaxation steps are distinguishable below 223 K; see Figure 1.

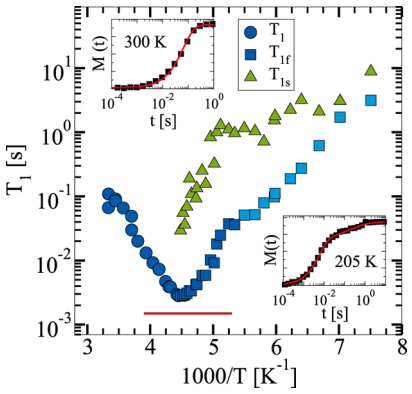

Figure 1. ^{2}H SLR times of D_2O in MCM-41 C10. While T_1 describes the exponential buildup of magnetization above 223 K, T_{1f} and T_{1s} are the time constants of the faster and slower relaxation steps below 223 K, respectively. Use of dark and light squares indicates that the faster relaxation step turns from a single exponential to a stretched exponential at 187 K. The line marks the minimum value for a Debye spectral density, T_{1D}, as calculated from eq 2 using the experimental values $\delta = 2\pi\cdot 161$ kHz and $\omega_0 = 2\pi\cdot 46.1$ MHz. The insets show the buildup of the magnetization $M(t)$ at (left) 300 and (right) 205 K in arbitrary units.

In the high-temperature range, T_1 is readily obtained from $M(t)$. T_1 is a minimum at 225 K, indicating $\tau \approx 1$ ns, but the minimum value is larger than that expected for a Debye process, $T_{1D} = 1.5$ ms. Thus, the correlation function of water reorientation is not a single exponential, consistent with a Cole−Cole (CC) spectral density in DS on H_2O in MCM.[10] A distribution $G(\log\tau)$ is expected, for example, due to diverse water dynamics in various pore regions.[5] Such distribution of correlation times τ should lead to a distribution of relaxation times T_1 and, hence, to nonexponential ^{2}H SLR. However, this argument is only true when the water molecules do not exchange their correlation times during the buildup of magnetization.[22] Consequently, our finding of exponential ^{2}H SLR above 223 K means that the assumption of time-independent correlation times is not valid, but the water molecules sample a representative set of local environments within the pore on the milliseconds time scale so that the corresponding exchange of τ values averages over any distribution of T_1 times and restores exponential ^{2}H SLR, resembling findings for the α process.[31]

In the low-temperature range, we fit the SLR functions $\Phi(t) = 1 - M(t)/M(\infty)$ to a weighted superposition of two stretched exponentials, $\exp[-(t/T_{1i})^{\beta_i}]$, where i = f and s denote the faster and slower relaxation steps, respectively. The faster step is exponential ($\beta_f = 1$) down to ∼187 K and $T_{1f}(T)$ continues to $T_1(T)$; see Figure 1. Hence, a fraction of water is still liquid and explores a substantial part of the pore volume below 223 K. The slower step is nonexponential ($\beta_s \approx 0.6$), and T_{1s} is about an order of magnitude longer than T_{1f}. These results imply that another fraction of water solidifies at about 223 K so that this species is less mobile and does not explore different environments, resulting in slower and nonexponential SLR. Coexistence of two relaxation steps indicates that the dynamically distinguishable fractions do not exchange water molecules on the time scale $T_{1s} \approx 1$ s, although the faster species can show $\tau \approx 1$ ns. Such absence of exchange is unlikely between coexisting liquid phases. Therefore, our NMR results together with calorimetry data[14,15] provide strong evidence that the internal water in MCM-41 C10 exists as a solid below 223 K, while the interfacial water is a liquid down to at least ∼187 K, where the faster step becomes nonexponential, too, and $T_{1f}(T)$ exhibits a kink.

Because quantitative analysis is straightforward for exponential SLR, we focus on the liquid fraction at $T > 187$ K. Motivated by DS results,[10] we use the CC spectral density

$$J_{cc}(\omega) = \frac{\omega^{-1}\sin\left(\frac{\pi}{2}\beta_c\right)(\omega\tau_c)^{\beta_c}}{1 + (\omega\tau_c)^{2\beta_c} + 2\cos\left(\frac{\pi}{2}\beta_c\right)(\omega\tau_c)^{\beta_c}} \quad (3)$$

Then, a width parameter $\beta_c = 0.65$ is obtained from the minimum value of T_1.[31] Exploiting that β_c is independent of temperature,[10] and by inserting $J_{cc}(\omega)$ into eq 2, we determine τ_c, corresponding to the mean logarithmic correlation time τ_m. In Figure 2, we see a crossover of τ_m at 220−230 K. Above, we find Vogel−Fulcher−Tammann (VFT) behavior, $\tau_m = \tau_0 \exp[B/(T - T_0)]$, in harmony with NS data.[9] Below, the SLR results no longer follow the NS data[9] but rather the DS data.[10] It deserves future attention whether probing of a diverse process or limitation of the time window causes the substantially different temperature dependence in NS work. Interestingly, both the change in water dynamics and the emergence of solid water occur at 220−230 K. Therefore, the crossover between VFT and ARR behaviors does not necessarily indicate a LL transition; see below.

In the following, we focus on the dynamics of liquid water at low temperatures. For this purpose, we suppress contributions from solid water to the measured signals based on the different SLR behavior. Specifically, partially relaxed (PR) experiments are performed, that is, we destroy the magnetization and start the measurement after a delay $T_{1f} \ll t \ll T_{1s}$ so that contributions from deuterons in the liquid and solid fractions are recovered to major and minor extents, respectively.

We start our studies on low-temperature liquid dynamics, performing ^{2}H LSA for PR spectra. In Figure 3a, we see that the PR spectrum is dominated by a narrow Lorentzian line above

dx.doi.org/10.1021/jz402539r | J. Phys. Chem. Lett. 2014, 5, 174−178

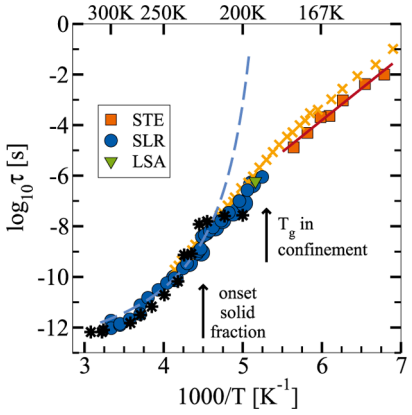

Figure 2. Correlation times of water dynamics in silica pores with diameters of about 2.0 nm. Mean logarithmic correlation times τ_m from the present SLR, LSA, and STE studies on D_2O in MCM-41 C10 are compared with DS results[10] (×) for H_2O in MCM-41 C10 and NS results[9] (*) for H_2O in MCM-41 15S. The SLR data for $T > 220$ K and the STE data for $T < 180$ K are interpolated with a VFT law (dashed line, $T_0 = 180$ K) and an Arrhenius law (solid line, $E_a = 0.50$ eV), respectively. The arrow at 187 K marks a calorimetric signature for H_2O in MCM-41 C10.[13]

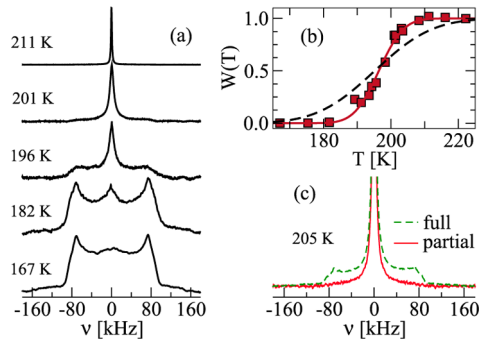

Figure 3. ^2H NMR solid-echo spectra of D_2O in MCM-41 C10. (a) Temperature-dependent spectra from PR experiments. (b) Relative contribution of the Lorentzian line, $W(T)$. The dashed line is an expectation calculated from DS data.[10] (c) Spectra obtained after partial and full relaxation at 205 K.

210 K and by a broad Pake spectrum below 180 K. The Lorentzian line indicates that the water molecules exhibit isotropic reorientation, which is fast on the time scale, $1/\delta \approx 1$ μs, and averages out the orientation dependence of ω_Q, confirming the liquid nature of the observed water species. The Pake shape, which results from the powder average, reveals that rotational motion of the water molecules no longer occurs on the experimental time scale. At intermediate temperatures, 180−210 K, the PR spectra of the liquid fraction can be described as a weighted superposition of Lorentzian and Pake components. This line shape is a consequence of the broad distribution $G(\log \tau)$, which results in coexistence of fast ($\tau \ll 1$ μs) and slow ($\tau \gg 1$ μs) water molecules, yielding the Lorentzian and Pake contributions, respectively. When the temperature is reduced, $G(\log \tau)$ shifts to longer times so that the fraction of fast molecules and the weighting factor of the Lorentzian, $W(T)$, continuously decrease, consistent with our observations. To check these arguments, we use the distribution obtained from DS[10] and calculate expectations for the contribution of the Lorentzian according to $W = \int_{-\infty}^{-6} G(\log \tau)\, d \log \tau$. In Figure 3b, we see fair agreement of the experimental and calculated weighting factors $W(T)$, confirming that a continuous slow down of broadly distributed dynamics of liquid water causes the observations. The transition region is narrower in the experimental data than that in the calculated data due to refocusing effects in the performed echo experiments,[25] as will be shown in future work. Figure 3c compares spectra obtained after partial relaxation and full relaxation at 205 K. Clearly, PR experiments enable suppression of the Pake contribution from solid water and provide access to the behavior of liquid water.

Finally, we combine ^2H STE with the PR technique to study ultraslow liquid dynamics. In ^2H STE, we correlate the frequencies ω_Q during two short evolution times $t_p \ll \tau$, separated by a longer mixing time $t_m \simeq \tau$ in the μs−ms range. Variation of t_m for fixed t_p provides access to the rotational correlation function[31]

$$F_2^{\cos}(t_m) \propto \langle \cos[\omega_Q(0)t_p] \cos[\omega_Q(t_m)t_p] \rangle \quad (4)$$

Here, $\langle ... \rangle$ denotes the ensemble average. In addition to water reorientation, spin relaxation damps the signal in experimental practice. Therefore, we analyze the normalized experimental data by fitting to

$$F_2^{\cos}(t_m) = \left[(1 - F_\infty) \exp\left[-\left(\frac{t_m}{\tau_k} \right)^{\beta_k} \right] + F_\infty \right] \Phi_f(t_m) \quad (5)$$

Hence, we describe the correlation loss due to water reorientation by a stretched exponential and use the residual correlation F_∞ to consider possible anisotropy. Also, we exploit that, in our PR experiments, additional damping is given by the SLR function of liquid water, $\Phi_f(t_m)$, which we determine in SLR measurements.

In Figure 4a, we see that $F_2^{\cos}(t_m)$ exhibits stretched decays, which shift to longer times upon cooling. These findings confirm that the Pake contribution in the PR spectra does not result from truly immobile molecules but from the slow part of a broad distribution $G(\log \tau)$. For a quantitative analysis, we interpolate the decays with eq 5 and calculate mean logarithmic correlation times τ_m according to $\ln \tau_m = (1 - 1/\beta_k)\mathrm{Eu} + \ln \tau_k$,

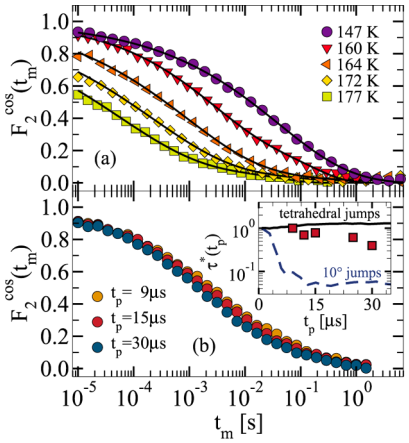

Figure 4. ^2H NMR STE decays for D_2O in MCM-41 C10. (a) Data for various temperatures and an evolution time $t_p = 9$ μs together with fits to eq 5. (b) Data for various evolution times t_p at 160 K. The inset shows the normalized time constant of the decays, $\tau^*(t_p) = \tau_k(t_p)/\tau_k(t_p \rightarrow 0)$, together with simulations for tetrahedral jumps and isotropic 10° jumps.[25]

dx.doi.org/10.1021/jz402539r | J. Phys. Chem. Lett. 2014, 5, 174−178

where Eu ≈ 0.58 is Euler's constant.[32] Inspection of Figure 2 reveals that these STE data are described by an ARR law with activation energy of $E_a \approx 0.50$ eV. Moreover, we see that the temperature dependence obtained from our STE study below 180 K is somewhat weaker than that resulting from our SLR and LSA approaches above 190 K, in agreement with findings in DS works.[10,11] Thus, ^{2}H NMR studies reveal *two* dynamic crossovers, one at 180−190 K and another at 220−230 K.

Finally, we use ^{2}H STE to ascertain the motional mechanism. The fits with eq 5 yield a residual correlation of $F_\infty \approx 0.14 \pm 0.10$. Hence, the observed low-temperature water reorientation does not result in a complete loss of correlation, that is, it is anisotropic rather than isotropic, indicating that it is not related to the α process but to the β process. To obtain further insights, we exploit the fact that $F_2(t_m)$ is independent of the used value of t_p when the reorientation results from large-angle jumps, for example, tetrahedral jumps, while it decays faster for longer evolution times when the reorientation involves small-angle jumps, resembling rotational diffusion.[31] In Figure 4b, it is evident that correlation functions for various evolution times t_p nearly coincide, indicating that water reorientation results from jumps about large angles on the order of the tetrahedral angle. Comparable behaviors were found for water dynamics at other surfaces,[24−28] while the α process exhibits a different mechanism.[31]

In conclusion, ^{2}H NMR proved to be a powerful tool to study D_2O in MCM-41 C10. The analysis revealed that liquid water exhibits a high-temperature crossover of rotational motion at 220−230 K, which coincides with an emergence of solid water, where, most probably, the liquid and solid fractions can be identified with interfacial and internal waters, respectively. Moreover, our studies unraveled that the liquid fraction shows a low-temperature crossover of reorientational dynamics at 180−190 K. While SLR and LSA results indicated that the orientation of individual molecules is subject to isotropic redistribution during an exploration of a substantial part of the interfacial region above this range, STE data clearly demonstrate that molecular reorientation is anisotropic below this range, suggesting that the reorganization of the water network ceases at 180−190 K.

These results imply the following scenario. Below 180−190 K, our STE studies probe the β process of water molecules near silica walls, which is anisotropic and localized, consistent with results for water dynamics in other confinements.[24−28] The low-temperature crossover reflects a change in the temperature dependence of the β process in response to a glass transition of interfacial water at T_g = 180−190 K, in harmony with a calorimetric signal in this temperature range.[13] Above T_g, the NMR results related to interfacial water continue to be governed by the β process up to 220−230 K due to a remarkably large amplitude of the underlying motion, but the α process restores ergodicity in the interface region, leading to exponential SLR. Two of our observations show that, in general, dynamic crossovers of confined water at ∼225 K do not yield evidence for a LL transition of bulk water, although the present results do not allow us to rule out this phenomenon, in particular, for high pressures. First, unlike in bulk liquids, an appearance of solid water, probably, freezing or vitrification[33] of internal water, accompanies the dynamic crossover of liquid water, indicating that the space available to the liquid fraction changes from 3D-like to 2D-like, that is, the interface region, at 220−230 K. Second, liquid water exhibits a prominent β process below ∼225 K, implying that a splitting of the β process from the α process contributes to changes in temperature-dependent correlation times in this range. Above 220−230 K, our NMR approach probes the α process of water molecules in all pore regions. Extrapolation of its VFT behavior to lower temperatures is consistent with $T_g \approx 190$ K (see Figure 2), but we cannot exclude that the temperature dependence of the α process changes when solid water forms. Altogether, our ^{2}H NMR study shows that liquid water in silica pores with diameters of ∼2 nm exhibits two dynamic crossovers, which are closely related to formation of crystalline or glassy water species. In future work, it may be worthwhile to study whether these results can be generalized to other confinements and aqueous mixtures.

■ ASSOCIATED CONTENT

Supporting Information

Parameters obtained from the various NMR analyses. This material is available free of charge via the Internet at http://pubs.acs.org.

■ AUTHOR INFORMATION

Corresponding Author

*E-mail: michael.vogel@physik.tu-darmstadt.de. Phone: +49 (0)6151 162933. Fax: +49 (0)6151 162833.

Notes

The authors declare no competing financial interest.

■ ACKNOWLEDGMENTS

We thank Jan Swenson (Chalmers University) for providing us with MCM-41 C10 and the Deutsche Forschungsgemeinschaft (Vo-905/9-1) for funding.

■ REFERENCES

(1) Poole, P. H.; Sciortino, F.; Essmann, U.; Stanley, H. E. Phase Behaviour of Metastable Water. *Nature* **1992**, *360*, 324−328.

(2) Mishima, O.; Stanley, H. E. The Relationship between Liquid, Supercooled and Glassy Water. *Nature* **1998**, *396*, 329−335.

(3) Ngai, K. L.; Capaccioli, S.; Thayyil, M. S.; Shinashiki, N. Resolution of Problems in Soft Matter Dynamics by Combining Calorimetry and Other Spectroscopies. *J. Therm. Anal. Calorim.* **2010**, *99*, 123−138.

(4) Scodinu, A.; Fourkas, J. T. Comparison of the Orientational Dynamics of Water Confined in Hydrophobic and Hydrophilic Nanopores. *J. Phys. Chem. B* **2002**, *106*, 10292−10295.

(5) Gallo, P.; Rovere, M.; Chen, S.-H. Dynamic Crossover in Supercooled Confined Water: Understanding Bulk Properties through Confinement. *J. Phys. Chem. Lett.* **2010**, *1*, 729−733.

(6) Erko, M.; Findenegg, G. H.; Cade, N.; Michette, A.; Paris, O. Confinement-Induced Structural Changes of Water Studied by Raman Scattering. *Phys. Rev. B* **2011**, *84*, 104205.

(7) Soper, A. K. Density Profile of Water Confined in Cylindrical Pores in MCM-41 Silica. *J. Phys.: Condens. Matter* **2012**, *24*, 064107.

(8) Yoshida, K.; Yamaguchi, T.; Kittaka, S.; Bellissent-Funel, M.-C.; Fouquet, P. Thermodynamic, Structural, and Dynamic Properties of Supercooled Water Confined in Mesoporous MCM-41 Studied with Calorimetric, Neutron Diffraction, and Neutron Spin Echo Measurements. *J. Chem. Phys.* **2008**, *129*, 054702.

(9) Liu, L.; Chen, S.-H.; Faraone, A.; Yen, C.-W.; Mou, C.-Y. Pressure Dependence of Fragile-to-Strong Transition and a Possible Second Critical Point in Supercooled Confined Water. *Phys. Rev. Lett.* **2005**, *95*, 117802.

(10) Sjöström, J.; Swenson, J.; Bergman, R.; Kittaka, S. Investigating Hydration Dependence of Dynamics of Confined Water: Monolayer, Hydration Water and Maxwell−Wagner Processes. *J. Chem. Phys.* **2008**, *128*, 154503.

(11) Bruni, F.; Mancinelli, R.; Ricci, M. A. Multiple Relaxation Processes Versus the Fragile-to-Strong Transition in Confined Water. *Phys. Chem. Chem. Phys.* **2011**, *13*, 19773−19779.
(12) Nagoe, A.; Kanke, Y.; Oguni, M.; Namba, S. Findings of C_p Maximum at 233 K for the Water within Silica Nanopores and Very Weak Dependence of the T_{max} on the Pore Size. *J. Phys. Chem. B* **2010**, *114*, 13940−13943.
(13) Kittaka, S.; Takahara, S.; Matsumoto, H.; Wada, Y.; Satoh, T. J.; Yamaguchi, T. Low Temperature Phase Properties of Water Confined in Mesoporous Silica MCM-41: Thermodynamic and Neutron Scattering Study. *J. Chem. Phys.* **2013**, *138*, 204714.
(14) Oguni, M.; Kanke, Y.; Nagoe, A.; Namba, S. Calorimetric Study of Water's Glass Transition in Nanoscale Confinement, Suggesting a Value of 210 K for Bulk Water. *J. Phys. Chem. B* **2011**, *115*, 14023−14029.
(15) Johari, G. P. Origin of the Enthalpy Features of Water in 1.8 nm Pores of MCM-41 and the Large C_p Increase at 210 K. *J. Chem. Phys.* **2009**, *130*, 124518.
(16) Vogel, M. NMR Studies on Simple Liquids in Confinement. *Eur. Phys. J.: Spec. Top.* **2010**, *189*, 47−64.
(17) Grünberg, B.; Emmler, T.; Gedat, E.; Shenderovich, I.; Findenegg, G. H.; Limbach, H.-H.; Buntkowsky, G. Hydrogen Bonding of Water Confined in Mesoporous Silica MCM-41 and SBA-15 Studied by ^{1}H Solid-State NMR. *Chem.—Eur. J.* **2004**, *10*, 5689−5696.
(18) Hansen, E. W.; Stocker, M.; Schmidt, R. Low-Temperature Phase Transition of Water Confined in Mesopores Probed by NMR. Influence on Pore Size Distribution. *J. Phys. Chem.* **1996**, *100*, 2195−2200.
(19) Mallamace, F.; Broccio, M.; Corsaro, C.; Faraone, A.; Wanderlingh, U.; Liu, L.; Mou, C.-Y.; Chen, S. H. The Fragile-to-Strong Dynamic Crossover Transition in Confined Water: Nuclear Magnetic Resonance Results. *J. Chem. Phys.* **2006**, *124*, 161102.
(20) Hwang, D. W.; Sinha, A. K.; Cheng, C.-Y.; Yu, T.-Y.; Hwang, L.-P. Water Dynamics on the Surface of MCM-41 via ^{2}H Double Quantum Filtered NMR and Relaxation Measurements. *J. Phys. Chem. B* **2001**, *103*, 5713−5721.
(21) Hassan, J.; Reardon, E.; Peemoeller, H. Correlation Between Deuterium NMR Spectral Components and MCM-41 Pore Surface Hydration Sites. *Microporous Mesorporous Mater.* **2009**, *122*, 121−127.
(22) Bodurka, J.; Buntkowsky, G.; Gutsze, A.; Limbach, H.-H. Evidence of Surface Diffusion of Water Molecules on Proteins of Rabbit Lens by ^{1}H NMR Relaxation Measurerments. *Z. Naturforsch.* **1996**, *51c*, 81−90.
(23) Febles, M.; Perez-Hernandez, N.; Perez, C.; Rodriguez, M. L.; Foces-Foces, C.; Roux, M. V.; Morales, E. Q.; Buntkowsky, G.; Limbach, H.-H.; Martin, J. D. Distinct Dynamic Behaviors of Water Molecules in Hydrated Pores. *J. Am. Chem. Soc.* **2006**, *128*, 10008−10009.
(24) Omichi, H.; Ueda, T.; Miyakubo, K.; Eguchi, T. Solid-State ^{2}H NMR Study of Nanocrystal Formation of D_2O and Their Dynamic Aspects in ACF Hydrophobic Nanospaces. *Chem. Lett.* **2007**, *36*, 256−257.
(25) Vogel, M. Origins of Apparent Fragile-to-Strong Transitions of Protein Hydration Waters. *Phys. Rev. Lett.* **2008**, *101*, 225701.
(26) Lusceac, S. A.; Vogel, M. R.; Herbers, C. R. ^{2}H and ^{13}C NMR Studies on the Temperature-Dependent Water and Protein Dynamics in Hydrated Elastin, Myoglobin and Collagen. *Biochim. Biophys. Acta, Proteins Proteomics* **2010**, *1804*, 41−48.
(27) Lusceac, S. A.; Vogel, M. ^{2}H NMR Study of the Water Dynamics in Hydrated Myoglobin. *J. Phys. Chem. B* **2010**, *114*, 10209−10216.
(28) Lusceac, S. A.; Rosenstihl, M.; Vogel, M.; Gainaru, C.; Fillmer, A.; Böhmer, R. NMR and Dielectric Studies of Hydrated Collagen and Elastin: Evidence for a Delocalized Secondary Relaxation. *J. Non-Cryst. Solids* **2011**, *357*, 655−663.
(29) Swenson, J.; Elamin, K.; Jansson, H.; Kittaka, S. Why Is There No Clear Glass Transition of Confined Water? *Chem. Phys.* **2013**, *424*, 20−25.
(30) Wittebort, R. J.; Usha, M. G.; Ruben, D. J.; Wemmer, D. E.; Pines, A. Observation of Molecular Reorientation in Ice by Proton and Deuterium Magnetic Resonance. *J. Am. Chem. Soc.* **1988**, *110*, 5668−5671.
(31) Böhmer, R.; Diezemann, G.; Hinze, G.; Rössler, E. Dynamics of Supercooled Liquids and Glassy Solids. *Prog. Nucl. Magn. Reson. Spectrosc.* **2001**, *39*, 191−267.
(32) Zorn, R. Logarithmic Moments of Relaxation Time Distributions. *J. Chem. Phys.* **2002**, *116*, 3204−3209.
(33) Swenson, J.; Teixeira, J. The Glass Transition and Relaxation Behavior of Bulk Water and a Possible Relation to Confined Water. *J. Chem. Phys.* **2010**, *132*, 014508.